Bragg Reflection Characteristics of Millimeter Waves in a Periodically Plasma-Induced Semiconductor Waveguide

MASAYUKI MATSUMOTO, MEMBER, IEEE, MAKOTO TSUTSUMI, MEMBER, IEEE, AND NOBUAKI KUMAGAI, FELLOW, IEEE

Abstract —**Theoretical analysis on the Bragg reflection characteristics of millimeter waves in a periodically plasma-induced semiconductor waveguide is presented. The plasma is assumed to be generated by light illumination. Numerical examples are given which show the dependence of the Bragg reflection characteristics on the length of the plasma-induced section and on the plasma density. Since the period can be changed by altering the illumination pattern, this type of periodic structure may be developed to tunable filters or tunable DBR oscillators for millimeter-wave region.**

RECENTLY, it has been suggested that high-resistivity semiconductors such as silicon and gallium arsenide be used as media for dielectric waveguides in millimeter-wave integrated circuits [1]. The use of semiconductors instead of insulators (alumina, for example) for waveguiding media has several advantages: 1) active devices such as IMPATT diodes can be directly incorporated with the waveguide, and 2) propagation characteristics of millimeter waves can be controlled by altering the electron-hole pair (plasma) density in the semiconductor. With regard to 2), very recently, Lee *et al.* [2] and Ogusu *et al.* [3] have examined to control the propagation characteristics of millimeter waves in a rectangular semiconductor waveguide making use of optical injection of plasma by illuminating the waveguide with above-bandgap radiation. In these papers, they have analyzed a semiconductor waveguide on whose surface plasma is induced uniformly along the propagation direction of millimeter waves, and have aimed at the application to optically controlled millimeter-wave phase shifters, switches, and modulators.

In this paper, we assume that a semiconductor slab waveguide is illuminated periodically in the direction of millimeter-wave propagation [4]. For such a periodic structure, we analyze theoretically the Bragg reflection characteristics of millimeter waves. The results obtained will be useful for designing tunable filters and tunable distributed Bragg reflector oscillators [5] for millimeter-wave region.

Manuscript received July 16, 1985; revised November 22, 1985.

The authors are with the Department of Communication Engineering, Faculty of Engineering, Osaka University, Yamada Oka, Suita, Osaka 565, Japan

IEEE Log Number 8407180.

II. Uniformly Plasma-Induced Semiconductor Waveguides

In this section, we describe the propagation characteristics of TE modes in a uniformly (along the propagation direction) plasma-induced semiconductor waveguide. Time dependence of the fields is assumed to be $\exp(j\omega t)$.

Fig. 1 shows the two-dimensional model of the semiconductor waveguide. It is assumed that the fields have no variation in the y direction and propagate in the z direction with the factor of $\exp(-j\beta z)$. Relative permittivity and the thickness of the semiconductor slab are ϵ_r and d, respectively. ϵ_r is a real quantity because the semiconductor is assumed to be intrinsic with very high resistivity. The lower surface of the semiconductor slab is illuminated with above-bandgap radiation and the plasma of uniform density is assumed to be induced in the region $0 < x < t_p$. Although it is desirable to treat a open-type waveguide for the application to millimeter-wave integrated circuits, we are concerned with the structure having two perfect-conducting walls above and below the semiconductor slab to avoid the complexity in analyzing the discontinuity problem due to the continuous nature of spectrum of open-type waveguides. The spacing between the semiconductor slab and the perfect-conducting walls is h.

Complex permittivity of the plasma-induced region $0 < x < t_p$ is given by [2]

$$\epsilon_p = \epsilon_r - \sum_{\iota = e,h} \frac{\omega_{p\iota}^2}{\omega^2 + \nu_\iota^2}\left(1 + j\frac{\nu_\iota}{\omega}\right)$$

where

$$\omega_{p\iota}^2 = \frac{nq^2}{\epsilon_0 m_\iota}$$

n, q, ϵ_0, ν_ι, and m_ι are plasma density, the elementary charge, permittivity of the free space, collision frequency, and effective mass of carrier, respectively. The subscripts e and h to ν and m refer to electron and hole, respectively. For silicon, $\epsilon_r = 11.8$, $\nu_e = 4.53 \times 10^{12}$ s^{-1}, $\nu_h = 7.71 \times 10^{12}$ s^{-1}, $m_e = 0.259\, m_0$, and $m_h = 0.38\, m_0$ (m_0 is the electron rest mass) [3]. These values are used in all the numerical

0018-9480/86/0400-0406$01.00 ©1986 IEEE

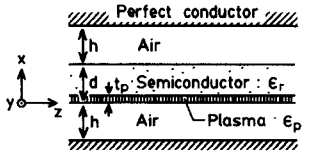

Fig. 1. Two-dimensional model of the plasma-induced semiconductor waveguide.

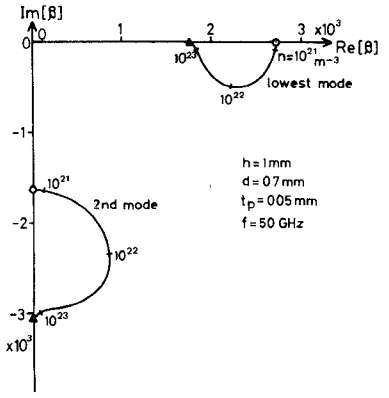

Fig. 2. Loci of the lowest two roots of the characteristic equation with varying the plasma density n.

calculations through this paper. In the frequency region around 50 GHz, the collision frequency ν_i is larger than the angular frequency ω of the electromagnetic fields about by an order, so the imaginary part of ϵ_p is mainly to be controlled by changing the plasma density n.

Characteristic equation of TE modes supported by the structure shown in Fig. 1 is given by

$$\left(1-\frac{k_p}{k_a}\tan k_a h \tan k_p t_p\right)\cdot\left\{\frac{1}{k_a}\tan k_a(h-d)+\frac{1}{k_d}\tan k_d(d-t_p)\right\}+\left(\frac{1}{k_p}\tan k_p t_p+\frac{1}{k_a}\tan k_a h\right)\cdot\left\{1-\frac{k_d}{k_a}\tan k_d(d-t_p)\tan k_a(h-d)\right\}=0 \quad (1a)$$

$$k_a=\left(\omega^2\epsilon_0\mu_0-\beta^2\right)^{1/2} \quad (1b)$$

$$k_d=\left(\omega^2\epsilon_0\mu_0\epsilon_r-\beta^2\right)^{1/2} \quad (1c)$$

$$k_p=\left(\omega^2\epsilon_0\mu_0\epsilon_p-\beta^2\right)^{1/2} \quad (1d)$$

where μ_0 is permiability of the free space. Fig. 2 shows the loci of the first two roots of equation (1) with varying the plasma density n from zero to infinity. Both roots start from the points ⊙ on the axes which indicate the values for the zero plasma density $n=0$, and after once leaving the axes, again approach to the axes with increasing the plasma density and end in the points △. The values indicated by △ can be also obtained by solving the characteristic equation with the plasma region replaced by the perfect conductor.

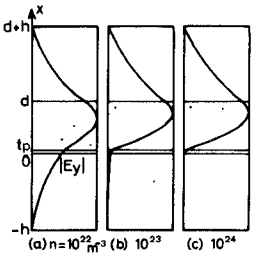

Fig. 3. Normalized field distributions of the dominant mode. ($h=1$ mm, $d=0.7$ mm, $t_p=0.05$ mm).

Fig. 3 shows the normalized electric field distributions of the dominant mode for three different values of n. Although it may be seen in this figure that the dominant-mode propagation is much affected by the presence of the two perfect-conducting walls, the value of propagation constant of the dominant mode, by which the center frequency in Bragg-reflector application is mainly determined, differs within 1.8 percent in relative value from the value for $h=\infty$. For $n=10^{22}$ and 10^{23} m^{-3}, the electromagnetic fields remain in the lossy plasma region as seen in Fig. 3(a) and (b), causing the large attenuation of the dominant mode. For $n=10^{24}$ m^{-3}, however, very little portion of the field exists in the plasma region as seen in Fig. 3(c), so the dominant mode suffers little loss. Therefore, using the optical illumination whose intensity is high enough to produce dense plasma as in Fig. 3(c), we can control millimeter-wave propagation by switching on or off the illumination without suffering large losses.

III. Discontinuity Problem

In this section, we present the analysis of the scattering problem at a discontinuous junction between intrinsic and plasma-induced semiconductor waveguides. The results will be employed to analyze a periodic structure in the later section.

Let the mth order mode of unit amplitude be incident upon the discontinuity between waveguide a (intrinsic semiconductor waveguide) and b (plasma-induced semiconductor waveguide) from waveguide a as shown in Fig. 4. The transverse components of the total electromagnetic fields in waveguides a and b at the discontinuity plane ($z=0$) can be approximately expressed in terms of finite number of eigenfunctions of waveguide a and b, respectively, as follows:

$$E_y^{(a)}(x)=E_{ym}^{(a)}(x)+\sum_{i=1}^{N}R_i E_{yi}^{(a)}(x)$$

$$H_x^{(a)}(x)=-\frac{1}{\omega\mu_0}\left\{\beta_m^{(a)}E_{ym}^{(a)}(x)-\sum_{i=1}^{N}R_i\beta_i^{(a)}E_{yi}^{(a)}(x)\right\}$$

$$E_y^{(b)}(x)=\sum_{i=1}^{N}T_i E_{yi}^{(b)}(x)$$

$$H_x^{(b)}(x)=-\frac{1}{\omega\mu_0}\sum_{i=1}^{N}T_i\beta_i^{(b)}E_{yi}^{(b)}(x)$$

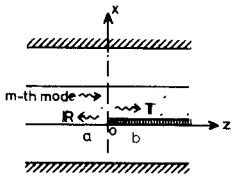

Fig. 4. Discontinuous junction between intrinsic and plasma-induced semiconductor waveguides.

where

$E_{yi}^{(p)}(x)$ eigenfunction of the ith mode in waveguide p ($p=a,b$),

$\beta_i^{(p)}$ propagation constant of the ith mode in waveguide p ($p=a,b$),

R_i reflection coefficient to the ith mode in waveguide a,

T_i transmission coefficient to the ith mode in waveguide b,

N number of modes in the field expansion in each waveguide,

and each eigenfunction is normalized according to

$$\int_{-h}^{d+h} |E_{yi}^{(p)}|^2\,dx = 1, \qquad i = 1 \sim N,\ p = a, b.$$

Next, the mean-square error to the boundary condition at the discontinuity plane is defined as [6], [7]

$$F = \frac{1}{2}\left(\frac{\int_{-h}^{d+h} |E_y^{(a)} - E_y^{(b)}|^2\,dx}{\int_{-h}^{d+h} |E_{ym}^{(a)}|^2\,dx} + \frac{\int_{-h}^{d+h} |H_x^{(a)} - H_x^{(b)}|^2\,dx}{\int_{-h}^{d+h} |H_{xm}^{(a)}|^2\,dx} \right). \tag{2}$$

The condition for which F becomes minimum is given by

$$\frac{\partial F}{\partial R_i^*} = 0, \qquad \frac{\partial F}{\partial T_i^*} = 0, \qquad i = 1 \sim N$$

resulting in a set of linear equations

$$\begin{pmatrix} \mathbb{D}_{11} & \mathbb{D}_{12} \\ \mathbb{D}_{21} & \mathbb{D}_{22} \end{pmatrix} \begin{pmatrix} \mathbb{R} \\ \mathbb{T} \end{pmatrix} = \begin{pmatrix} \mathbb{C}_1 \\ \mathbb{C}_2 \end{pmatrix} \tag{3}$$

where $\mathbb{D}_{ij}$ ($i, j = 1,2$) are matrices of order N, $\mathbb{C}_i$ ($i = 1,2$) are column vectors of N components, and

$$\mathbb{R} = [R_1, R_2, \cdots, R_N]^t$$

$$\mathbb{T} = [T_1, T_2, \cdots, T_N]^t.$$

The detailed expressions for the elements of $\mathbb{D}_{ij}$ and $\mathbb{C}_i$ are given in Appendix. By solving (3), reflection and transmission coefficients in case of the mth mode incidence from waveguide a can be obtained. Those coefficients in case of the mth mode incidence from waveguide b can be also obtained in a similar way.

Table I shows numerical examples for the minimum value of F which is given by substituting the solution of (3) into (2). The minimum value of F decreases monotonically to zero with increasing the number of modes N.

TABLE I
NUMERICAL EXAMPLES FOR THE MINIMUM VALUE OF F ($h = 1$ mm, $d = 0.7$ mm, $t_p = 0.03$ mm, $n = 10^{24}$ m^{-3})

N	F (dominant mode incidence from waveguide a)	F (dominant mode incidence from waveguide b)
5	8.095 %	6.111 %
10	4.132	2.577
20	1.909	1.145
40	0.802	0.452
80	0.290	0.158
160	0.163	0.090

IV. Periodically Plasma-Induced Semiconductor Waveguides

A. Reflection Coefficient from the Periodic Structure

Fig. 5 shows a periodically plasma-induced semiconductor waveguide which consists of cascaded discontinuous junctions. Although an infinite number of modes are excited at each discontinuity, all of the modes do not interact appreciably with adjacent discontinuities. The number of modes which cause appreciable interaction with adjacent discontinuities (these modes are called "accessible modes" [8]) is assumed to be M_a and M_b in the waveguide a and b, respectively.

Equation (3) is solved $M_a + M_b$ times with each of the accessible modes taken to be incident upon the discontinuity. Each solution has the form of a column vector of $2N$ components. After truncating the each solution to a column vector of $M_a + M_b$ components, they can be arranged as vectors in a matrix form. Then, we obtain the scattering matrix $\mathbb{S}$ of order $M_a + M_b$ between accessible modes. The following relation holds.

$$\begin{pmatrix} \mathbb{A}^- \\ \mathbb{B}^+ \end{pmatrix} = \mathbb{S} \begin{pmatrix} \mathbb{A}^+ \\ \mathbb{B}^- \end{pmatrix}, \qquad \mathbb{S} \triangleq \begin{pmatrix} \mathbb{S}_{11} & \mathbb{S}_{12} \\ \mathbb{S}_{21} & \mathbb{S}_{22} \end{pmatrix},$$

where $\mathbb{A}^{\pm}$ ($\mathbb{B}^{\pm}$) are column vectors of M_a (M_b) components consisting of complex amplitudes of the lowest to M_ath (M_bth) order eigenmodes traveling in $\pm z$ directions in waveguide $a(b)$, and $\mathbb{S}_{11}$, $\mathbb{S}_{12}$, $\mathbb{S}_{21}$, and $\mathbb{S}_{22}$ are matrices of $M_a \times M_a$, $M_a \times M_b$, $M_b \times M_a$, and $M_b \times M_b$, respectively. The transfer matrix of a unit cell of the periodic structure shown in Fig. 6 can be expressed in terms of $\mathbb{S}_{ij}$ ($i, j = 1,2$):

$$\begin{pmatrix} \mathbb{A}^+ & (\Lambda_b) \\ \mathbb{A}^- & (\Lambda_b) \end{pmatrix} = \mathbb{G} \begin{pmatrix} \mathbb{A}^+ & (-\Lambda_a) \\ \mathbb{A}^- & (-\Lambda_a) \end{pmatrix}, \qquad \mathbb{G} \triangleq \begin{pmatrix} \mathbb{G}_{11} & \mathbb{G}_{12} \\ \mathbb{G}_{21} & \mathbb{G}_{22} \end{pmatrix}$$

$$\mathbb{G}_{11} = (\mathbb{P} - \mathbb{Q}\mathbb{P}^{-1}\mathbb{Q})\mathbb{D}_a, \qquad \mathbb{G}_{12} = \mathbb{Q}\mathbb{P}^{-1}\mathbb{D}_a^{-1}$$

$$\mathbb{G}_{21} = -\mathbb{P}^{-1}\mathbb{Q}\mathbb{D}_a, \qquad \mathbb{G}_{22} = \mathbb{P}^{-1}\mathbb{D}_a^{-1}$$

$$\mathbb{P} = \mathbb{S}_{12}\left(\mathbb{D}_b^{-1} - \mathbb{S}_{22}\mathbb{D}_b\mathbb{S}_{22}\right)^{-1}\mathbb{S}_{21}$$

$$\mathbb{Q} = \mathbb{S}_{11} + \mathbb{S}_{12}\left(\mathbb{D}_b^{-1} - \mathbb{S}_{22}\mathbb{D}_b\mathbb{S}_{22}\right)^{-1}\mathbb{S}_{22}\mathbb{D}_b\mathbb{S}_{21}$$

$$\mathbb{D}_a = \operatorname{diag}\left[\exp\left(-j\beta_1^{(a)}\Lambda_a\right), \exp\left(-j\beta_2^{(a)}\Lambda_a\right), \cdots, \exp\left(-j\beta_{Ma}^{(a)}\Lambda_a\right)\right]$$

$$\mathbb{D}_b = \operatorname{diag}\left[\exp\left(-j\beta_1^{(b)}\Lambda_b\right), \exp\left(-j\beta_2^{(b)}\Lambda_b\right), \cdots, \exp\left(-j\beta_{M_b}^{(b)}\Lambda_b\right)\right]$$

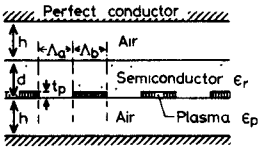

Fig. 5. Periodically plasma-induced semiconductor waveguide.

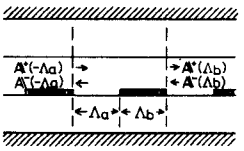

Fig. 6. Unit cell of the periodic structure.

(diag[ ] means a diagonal matrix whose diagonal elements are given in the bracket.) where Λ_a and Λ_b are the length of a section of waveguide a and b, respectively. The transfer matrix of the periodic structure consisting of N_c unit cells is given by $\mathbb{G}^{N_c}$. The reflection coefficient of the dominant mode from the structure can be calculated by

$$r = -\left(\tilde{\mathbb{G}}_{22}^{-1}\tilde{\mathbb{G}}_{21}\right)_{11}$$

where $\tilde{\mathbb{G}}_{ij}$ are submatrices of order M_a of G^{N_c} as

$$\mathbb{G}^{N_c} \triangleq \begin{pmatrix} \tilde{\mathbb{G}}_{11} & \tilde{\mathbb{G}}_{12} \\ \tilde{\mathbb{G}}_{21} & \tilde{\mathbb{G}}_{22} \end{pmatrix}.$$

B. Numerical Results

Fig. 7(a) and (b) show the reflection coefficients of the dominant mode from a pair of discontinuities depicted in the insets of the figures as functions of the assumed number of the accessible modes M_b and M_a. Distances between the two discontinuities Λ_b and Λ_a serve as parameters. The number of expansion modes N in the analysis of an individual discontinuity is chosen to be 50 in all the numerical calculations in this section. It can be seen in Fig. 7(a) and (b) that the convergence of the reflection coefficients with increasing M_b and M_a is slower for smaller distances Λ_b and Λ_a, respectively. That is, larger number of modes interact appreciably with adjacent discontinuities for smaller distance between the discontinuities. Using these figures, we can determine the number of accessible modes in each section of waveguide a and b for particular values of Λ_a and Λ_b of the periodic structure to be analyzed.

Fig. 8 shows the Bragg reflection characteristic of the periodic structure: $h = 1$ mm, $d = 0.7$ mm, $t_p = 0.03$ mm, $n = 10^{24}$ m^{-3}, $\Lambda_a = \Lambda_b = 0.68$ mm, $N_c = 20$. For this waveguide dimension, the number of propagation modes is only one in each section of waveguide a and b. (Since the propagation constants β of eigenmodes in waveguide b have complex values, we cannot classify these modes into propagation and evanescent modes. However, the modes whose β satisfies the inequality $\mathrm{Re}[\beta] \gg \mathrm{Im}[\beta]$ may be regarded as a propagation mode.) In this figure, we also show the Bragg reflection characteristic for $h = 2$ mm to examine the influence of the presence of perfect-conducting walls. In this case, the dominant-mode propagation

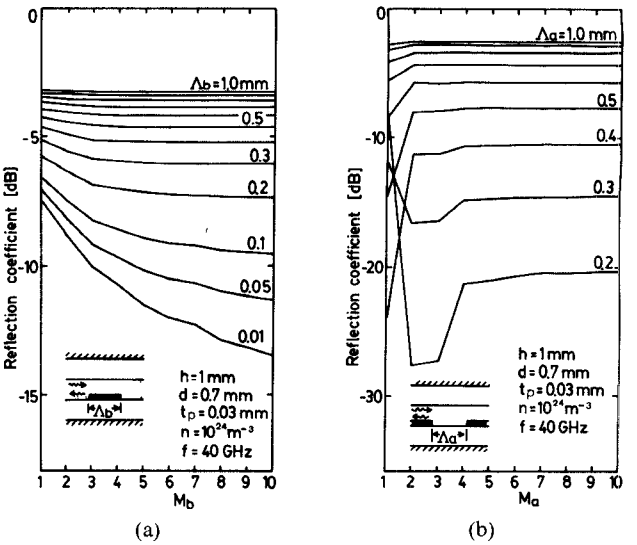

Fig. 7. Reflection coefficients of the dominant mode from a pair of discontinuities versus assumed number of the accessible modes. (a) With waveguide b between discontinuities. (b) With waveguide a between discontinuities.

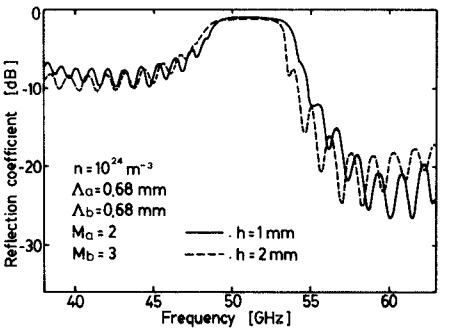

Fig. 8. Bragg reflection characteristics. ($d = 0.7$ mm, $t_p = 0.03$ mm, $N_c = 20$).

constant at 50 GHz differs within 0.06 percent from that of the open-type structure. Bragg reflection characteristics for $h = 1$ mm and $h = 2$ mm are qualitatively the same, which indicates that we can infer to a considerable extent the Bragg reflection characteristics of the open-type structure from those for $h = 1$ mm.

In Fig. 8, it should be noted that considerable reflection occurs in the low frequency region of 38–48 GHz compared with the high frequency region of 55–63 GHz. The reason seems to be as follows: reflected power by a discontinuity is large in the low frequency region near the cutoff frequency of the dominant mode in waveguide b, and the incident power of the dominant mode cannot penetrate deep into the periodic structure, so that the reflected waves from discontinuities do not cancel each other effectively in this frequency region. The amount of reflected power per unit cell can be decreased by shortening the length of the plasma-induced section Λ_b. This is also desirable in view of saving energy of illumination to generate the plasma. Fig. 9 shows the Bragg reflection characteristic for $\Lambda_a = 1.13$ mm and $\Lambda_b = 0.03$ mm. Reflected power in the low frequency region is reduced compared with Fig. 8.

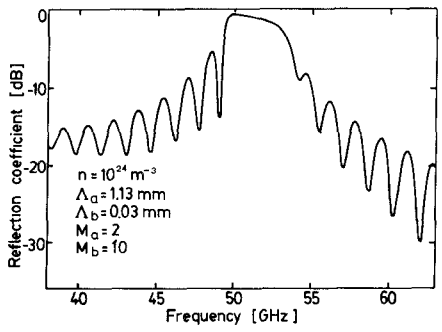

Fig. 9. Bragg reflection characteristic for small Λ_b. ($h = 1$ mm, $d = 0.7$ mm, $t_p = 0.03$ mm, $N_c = 20$).

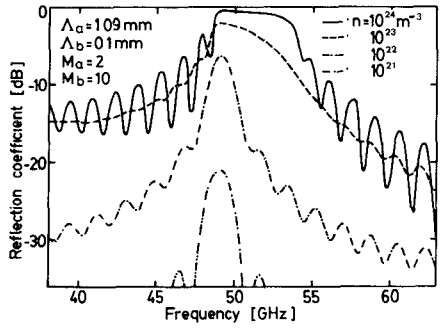

Fig. 10. Dependence of Bragg reflection characteristics on the plasma density n. ($h = 1$ mm, $d = 0.7$ mm, $t_p = 0.03$ mm, $N_c = 20$).

Fig. 10 shows the dependence of Bragg reflection characteristics on the plasma density in waveguide b. The peak value of reflected power is larger for higher plasma density. This is mainly because the dominant mode in waveguide b suffers smaller losses by the plasma for higher plasma density as stated in Section II.

To conclude this section, we make an estimation of the value of optical intensity required for device operation. Assuming that all of the optical energy is absorbed in the semiconductor and that the quantum efficiency is 100 percent, we can estimate optical intensity required to produce the steady-state plasma layer of density n and thickness t_p by

$$I = \frac{\hbar \omega_{\text{opt}} n t_p}{\tau}$$

where $\hbar$, ω_{opt}, and τ are Plank's constant divided by 2π, angular frequency of the optical radiation, and lifetime of the plasma, respectively. The value of I for $\lambda_{\text{opt}} = 2\pi/(\omega_{\text{opt}}\sqrt{\epsilon_0 \mu_0}) = 0.9$ μm, $n = 10^{24}$ m^{-3}, $t_p = 0.03$ mm, and $\tau = 2$ μs [4] is calculated to be 3.3×10^2 W/cm^2. To realize a Bragg reflector whose width (in the y direction in Fig. 1), Λ_b, and N_c are 3 mm, 0.1 mm, and 20, respectively, total optical power of 20 W is required. Although this value of optical power would be achieved by a N_d:YAG laser system, it is somewhat large to be provided by present-day semiconductor lasers [9]. In above estimation, steady-state thickness of the plasma layer is taken to be 30 μm which is approximately equal to optical penetration depth. In reality, however, the volume of the plasma-occupied region expands by carrier diffusion (ambipolar diffusion length in silicon is about 67 μm for $\tau = 2$ μs at 300K) so that more optical power will be required than estimated above. In order to confine the plasma in a thin layer, a structure of a dielectric waveguide covered with a thin semiconductor layer [10] will be preferable.

V. Conclusions

We have analyzed theoretically the Bragg reflection characteristics of millimeter waves in a periodically plasma-induced semiconductor waveguide assuming that a semiconductor slab is illuminated periodically with above-bandgap radiation. Some numerical examples are presented which show the dependence of the Bragg reflection characteristics on the length of the plasma-induced section and on the plasma density. In this paper, we have analyzed only the case of TE polarization. Calculation for TM polarization is now in progress.

The analysis in this paper assumes the presence of perfect-conducting walls above and below the semiconductor slab. However, if the spacing between the perfect-conducting walls and the semiconductor slab is not extremely small, the propagation characteristics of the dominant mode of the closed-type structure are nearly identical to those of the open-type structure. Hence, most of the results obtained in this paper can be also applied to the open-type structure apart from the influence of radiation losses.

Since the periodic loading with light-induced plasma treated in this paper is not permanent, this type of periodic structure can be developed to operate as tunable filters or tunable DBR oscillators for millimeter-wave region, although in order to produce a steady-state high-density plasma we need to solve problems of obtaining a high-power light source and of excess heating of the material.

Finally, it is mentioned that the analysis method and the results presented in this paper can be also applied to the case of periodically heavily doped semiconductor waveguides.

Appendix

The elements of $\mathbb{D}_{ij}$ and $\mathbb{C}_i$ in (3) are given by

$$(\mathbb{D}_{11})_{ij} = \left(1 + \frac{\beta_j^{(a)}\beta_i^{(a)*}}{|\beta_m^{(a)}|^2}\right)\int_{-h}^{d+h} E_{yj}^{(a)} E_{yi}^{(a)*}\, dx = \left(1 + \frac{|\beta_i^{(a)}|^2}{|\beta_m^{(a)}|^2}\right)\delta_{ij}$$

$$(\mathbb{D}_{12})_{ij} = -\left(1 - \frac{\beta_j^{(b)}\beta_i^{(a)*}}{|\beta_m^{(a)}|^2}\right)\int_{-h}^{d+h} E_{yj}^{(b)} E_{yi}^{(a)*}\, dx$$

$$(\mathbb{D}_{21})_{ij} = (\mathbb{D}_{12})_{ji}^*$$

$$(\mathbb{D}_{22})_{ij} = \left(1 + \frac{\beta_j^{(b)}\beta_i^{(b)*}}{|\beta_m^{(a)}|^2}\right)\int_{-h}^{d+h} E_{yj}^{(b)} E_{yi}^{(b)*}\, dx$$

$$(\mathbb{C}_1)_i = -\left(1 - \frac{\beta_i^{(a)*}}{\beta_m^{(a)*}}\right)\int_{-h}^{d+h} E_{ym}^{(a)} E_{yi}^{(a)*}\, dx = 0$$

$$(\mathbb{C}_2)_i = \left(1 + \frac{\beta_i^{(b)*}}{\beta_m^{(a)*}}\right)\int_{-h}^{d+h} E_{ym}^{(a)} E_{yi}^{(b)*}\, dx$$

where δ_{ij} is the Kronecker delta. It should be noted that the eigenfunctions of waveguide b are not orthogonal among each other because it contains a lossy medium. Hence the matrix $\mathbb{D}_{22}$ is not a diagonal one as $\mathbb{D}_{11}$.

ACKNOWLEDGMENT

The authors wish to thank H. Shimasaki of Osaka University for his assistance in this work.

REFERENCES

[1] H. Jacobs and M. M. Chrepta, "Electronic phase shifter for millimeter-wave semiconductor dielectric integrated circuits," *IEEE Trans. Microwave Theory Tech.*, vol. MTT-22, pp. 411–417, Apr. 1974.

[2] C. H. Lee, P. S. Mak, and A. P. Defonzo, "Optical control of millimeter-wave propagation in dielectric waveguides," *IEEE J. Quantum Electron.*, vol. QE-16, pp. 277–288, Mar. 1980.

[3] K. Ogusu, I. Tanaka, and H. Itoh, "Propagation properties of dielectric waveguides with optically induced plasma layers," *Trans. IECE Japan*, vol. J66-C, pp. 39–46, Jan. 1983.

[4] R. Karg and E. Kreutzer, "Light-controlled semiconductor waveguide antenna," *Electron. Lett.*, vol. 13, no. 9, pp. 246–247, Apr. 1977.

[5] T. Itoh and F. J. Hsu, "Distributed Bragg reflector Gunn oscillators for dielectric millimeter-wave integrated circuits," *IEEE Trans. Microwave Theory Tech.*, vol. MTT-27, pp. 514–518, May 1979.

[6] M. Tsuji, H. Shigesawa, and K. Takiyama, "Transmission characteristics of partially corrugated dielectric loaded waveguides," IECE Japan, Technical Group Paper MW 84-10, Apr. 1984.

[7] J. B. Davies, "A least-squares boundary residual method for the numerical solution of scattering problems," *IEEE Trans. Microwave Theory Tech.*, vol. MTT-21, pp. 99–104, Feb. 1973.

[8] T. E. Rozzi and W. F. G. Mecklenbräuker, "Wide-band network modeling of interacting inductive irises and steps," *IEEE Trans. Microwave Theory Tech.*, vol. MTT-23, pp. 235–245, Feb. 1975.

[9] D. R. Scifres, C. Lindström, R. D. Burnham, W. Streifer and T. L. Paoli, "Phase-locked (GaAl)As laser diode emitting 2.6W CW from a single mirror," *Electron. Lett.*, vol. 19, no. 5, pp. 169–171, Mar. 1983.

[10] K. Ogusu and I. Tanaka, "Dielectric waveguide-type millimeter-wave modulator using photoconductivity," *Trans. IECE Japan*, vol. J67-B, pp. 416–423, Apr. 1984.

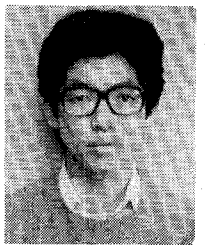

Masayuki Matsumoto (M'85) was born in Osaka, Japan, on January 6, 1960. He received the B.S. and M.S. degrees in engineering from Osaka University, Suita, Osaka, Japan, in 1982 and 1984, respectively.

Since 1985, he has been with the Department of Communication Engineering, Osaka University, where he has been engaged in research work on millimeter-wave integrated circuits and components.

Mr. Matsumoto is a member of the Institute of Electronics and Communication Engineers of Japan.

Makoto Tsutsumi (M'71) was born in Tokyo, Japan, on February 25, 1937. He received the B.S. degree in electrical engineering from Ritsumeikan University, Kyoto, in 1961, and the M.S. and Ph.D. degrees in communication engineering from Osaka University, Osaka, Japan, in 1963 and 1971, respectively.

From 1974 to 1983, he was a Lecturer, and has been an Associate Professor of Communication Engineering at Osaka University since 1984.

His current research areas include microwave and millimeter wave ferrite devices.

Dr. Tsutsumi is a member of the Institute of Electronics and Communication Engineers of Japan and Japan Society of Applied Physics.

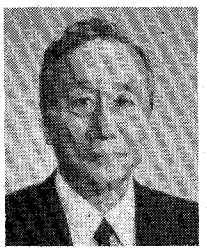

Nobuaki Kumagai (M'59–SM'71–F'81) was born in Ryojun, Japan, on May 19, 1929. He received the B. Eng. and D. Eng. degrees from Osaka University, Osaka, Japan, in 1953 and 1959, respectively.

From 1956 to 1960, he was a Research Associate in the Department of Communication Engineering at Osaka University. From 1958 through 1960, he was a Visiting Senior Research Fellow at the Electronics Research Laboratory of the University of California, Berkeley, while on leave of absence from Osaka University. From 1960 to 1970, he was an Associate Professor of Communication Engineering at Osaka University, and became Professor in 1971. From 1980 to 1982, he served as Dean of Students of Osaka University. From April of 1985, he was Dean of Engineering of Osaka University, and has been a President of Osaka University since August of 1985.

His fields of interest are electromagnetic theory and its applications to the microwaves, millimeter-waves, and acoustic-waves engineering, optical fibers and related techniques, and Lasers and their applications. He has published more than one hundred technical papers on these topics in established journals. He is the author or coauthor of several books including *Microwave Circuits* and *Introduction to Relativistic Electromagnetic Field Theory*. From 1971 to 1981, he was Chairman of the technical group on Microwave Theory and Techniques of the Institute of Electronics and Communication Engineers of Japan. He is a member of the Telecommunications Technology Council of the Ministry of Post and Telecommunications and is a consultant for the Nippon Telegraph and Telephone Corporation (NTT).

Dr. Kumagai is Vice President of the Institute of Electronics and Communication Engineers of Japan, member of the Institute of Electrical Engineers of Japan and of the Laser Society of Japan. He has received the Achievement Award from the Institute of Electronics and Communication Engineers of Japan and the Special Award from Laser Society of Japan. He was also awarded an IEEE Fellowship for contributions to the study of wave propagation in electromagnetics, optics, and acoustics.